Electronic Supplementary Material (ESI) for Journal of Materials Chemistry A.

Supporting Information

Improving the mechanical stability of zirconium-based metal-organic frameworks by incorporation of acidic modulators

Ben Van De Voorde,[a] Ivo Stassen,[a] Bart Bueken,[a] Frederik Vermoortele,[a] Dirk De Vos,[a] Rob Ameloot,[a] Jin-Chong Tan[b,*] and Thomas D. Bennett[c,*]

[a]Centre for Surface Chemistry and Catalysis, KU Leuven, Arenbergpark 23, B-3001 Leuven, Belgium.

[b]Department of Engineering Science, University of Oxford, Parks Road, Oxford OX1 3PJ, United Kingdom.

[c]Department of Materials Science and Metallurgy, University of Cambridge, Cambridge CB3 0FS, United Kingdom.

SI-1: Modulated sample characterization

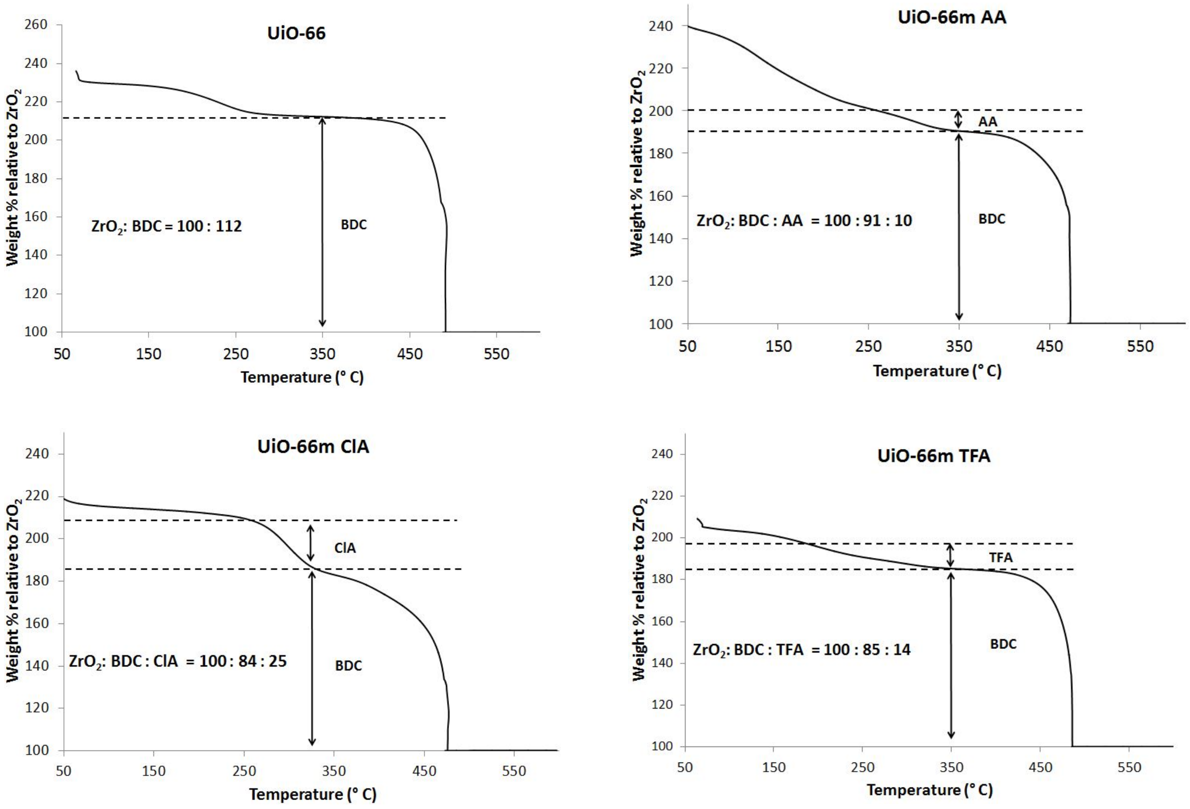

Figure S1. Additional thermogravimetric analyses were performed to analyze the linker deficiency of each UiO-66 material by heating the samples at 3°C / min under an oxygen containing atmosphere. Weights were normalized with respect to the ZrO_2 residue left after heating up to 550°C.

SI-2: Powder X-ray diffraction

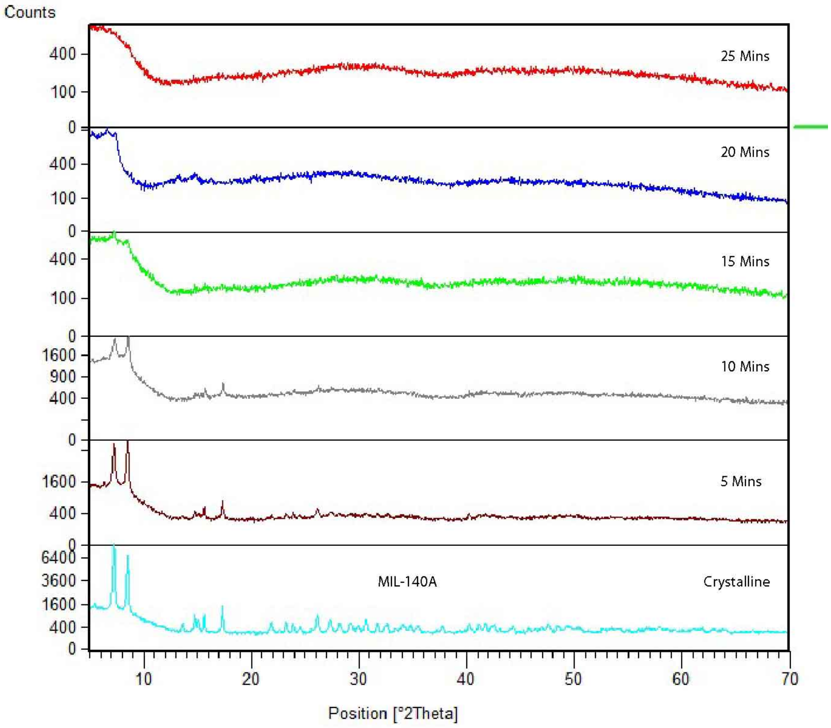

Figure S2a. Powder X-ray diffraction patterns of MIL-140A after milling for the indicated lengths of time.

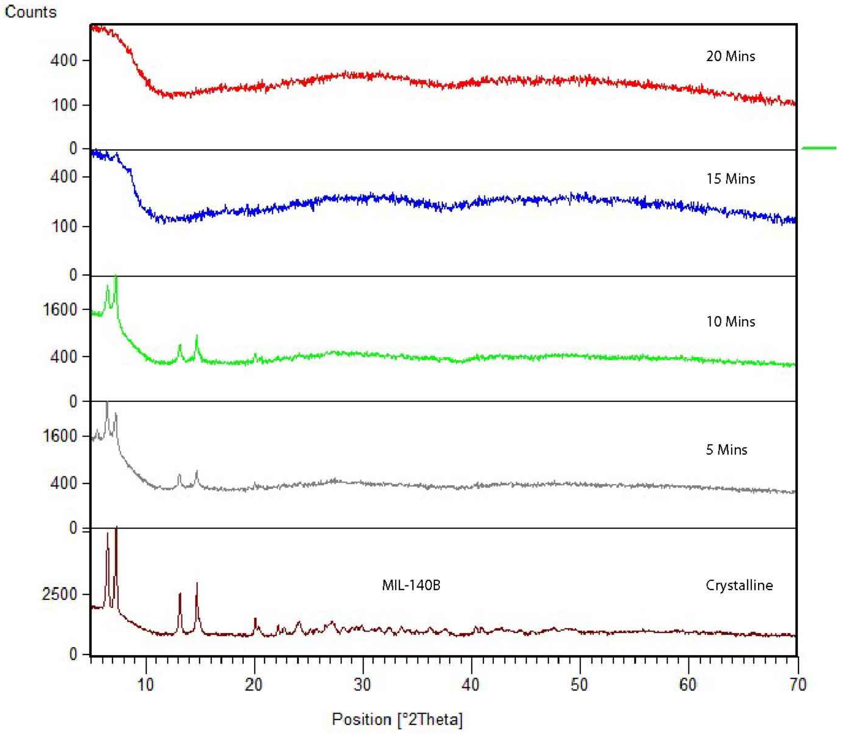

Figure S2b. Powder X-ray diffraction patterns of MIL-140B after milling for the indicated lengths of time.

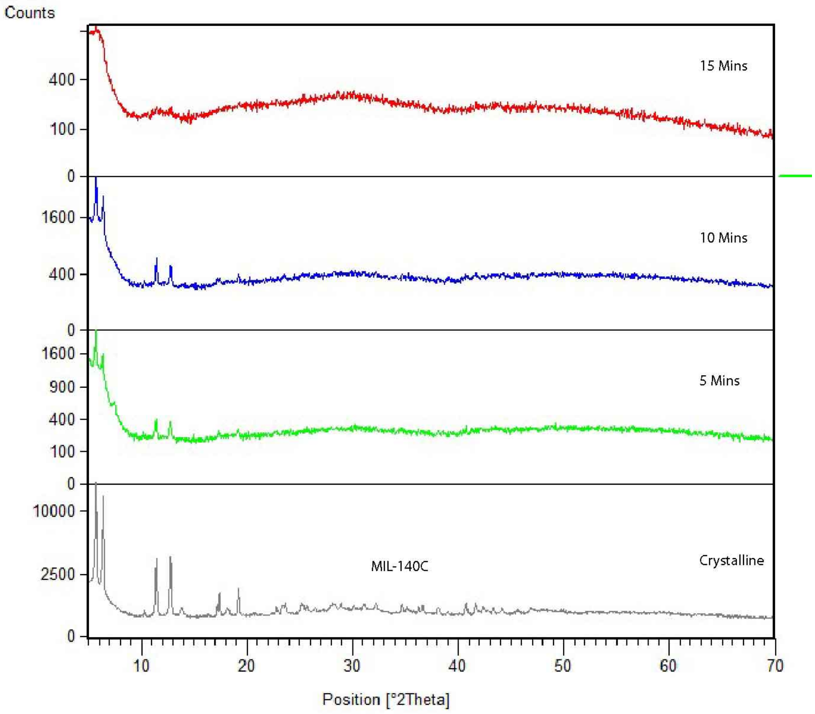

Figure S2c. Powder X-ray diffraction patterns of MIL-140C after milling for the indicated lengths of time.

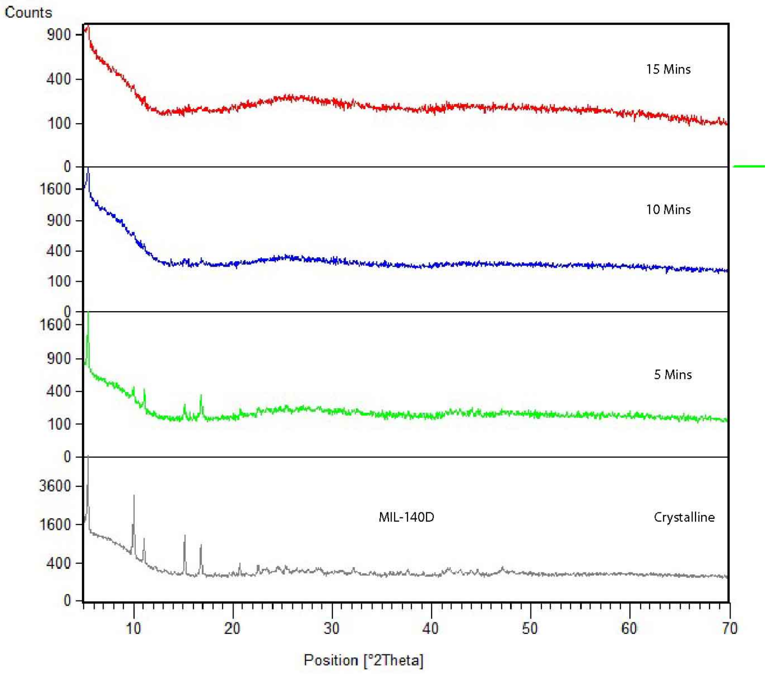

Figure S2d. Powder X-ray diffraction patterns of MIL-140D after milling for the indicated lengths of time.

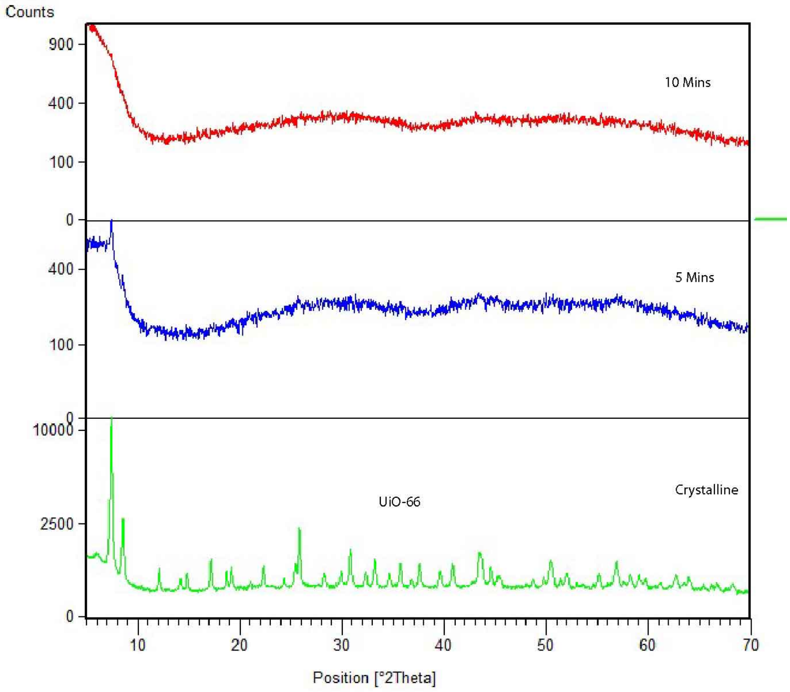

Figure S2e. Powder X-ray diffraction patterns of UiO-66 after milling for the indicated lengths of time.

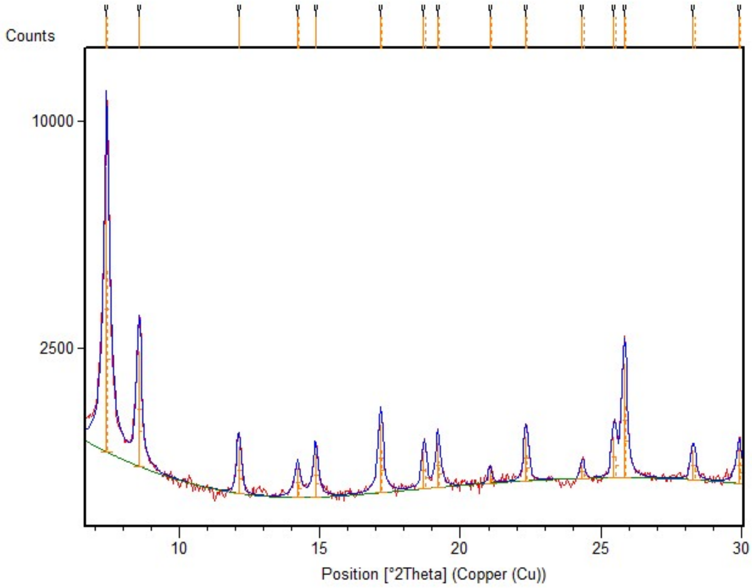

Figure S2f. Example of profile fitting for crystalline UiO-66.

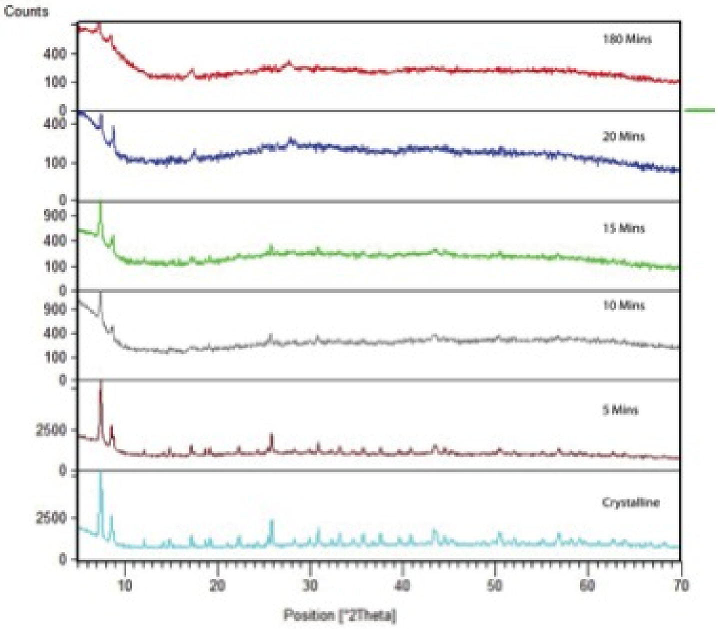

Figure S2g. Powder X-ray diffraction patterns of UiO-66m TFA after milling for the indicated lengths of time.

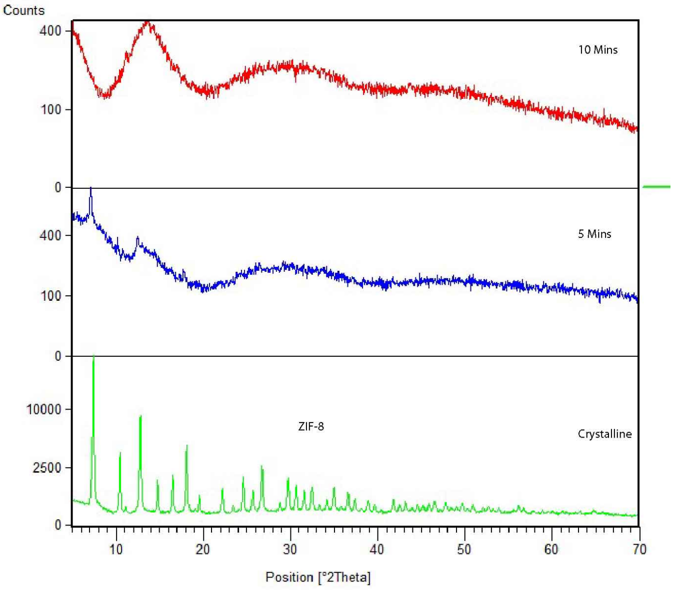

Figure S2h. Powder X-ray diffraction patterns of ZIF-8 after milling for the indicated lengths of time.

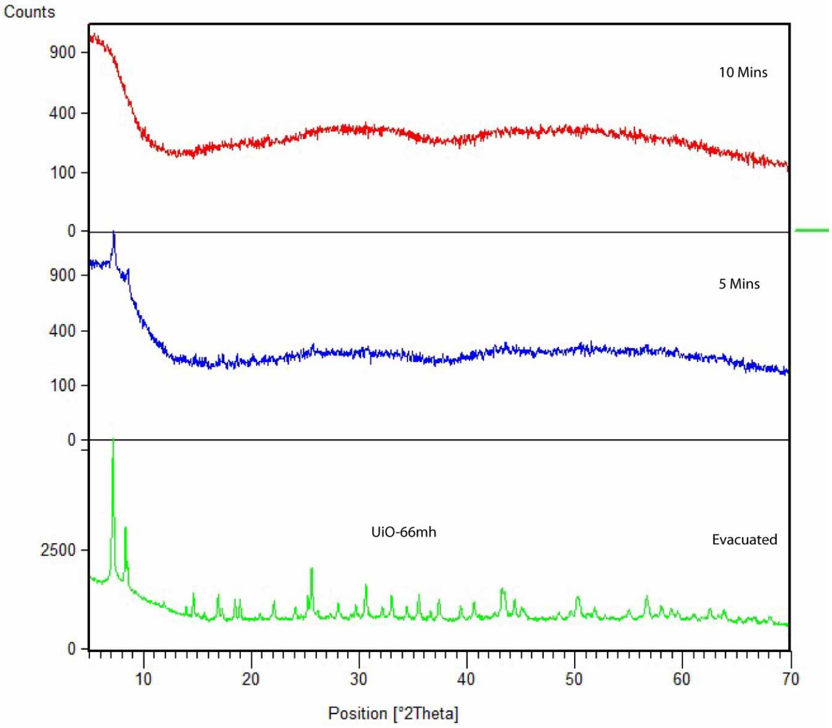

Figure S2i. Powder X-ray diffraction patterns of UiO-66mh after milling for the indicated lengths of time.

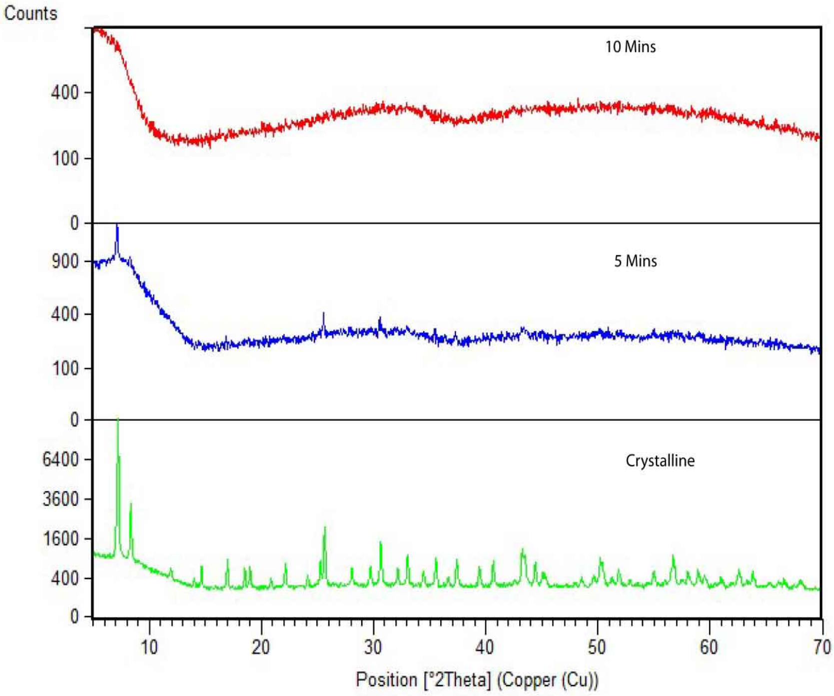

Figure S2j. Powder X-ray diffraction patterns of UiO-66m ClA after milling for the indicated lengths of time.

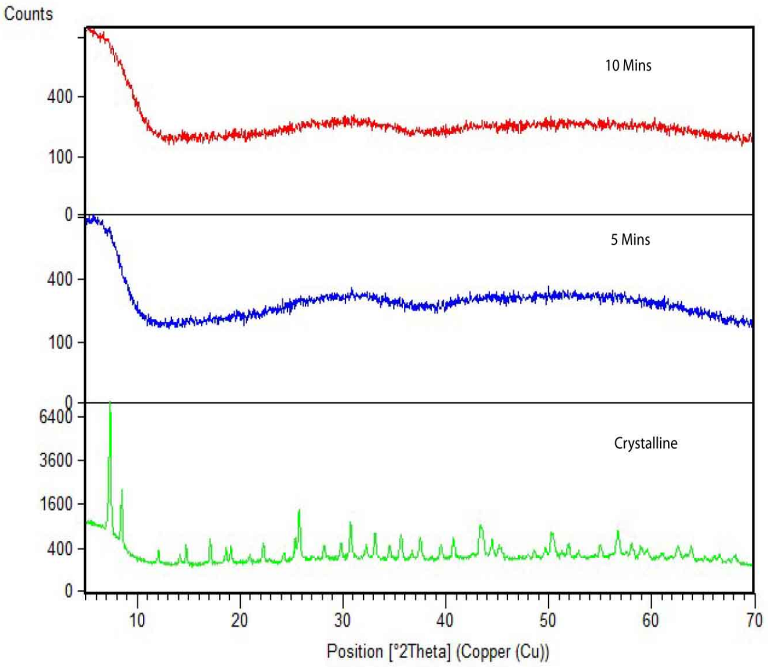

Figure S2k. Powder X-ray diffraction patterns of UiO-66m AA after milling for the indicated lengths of time.

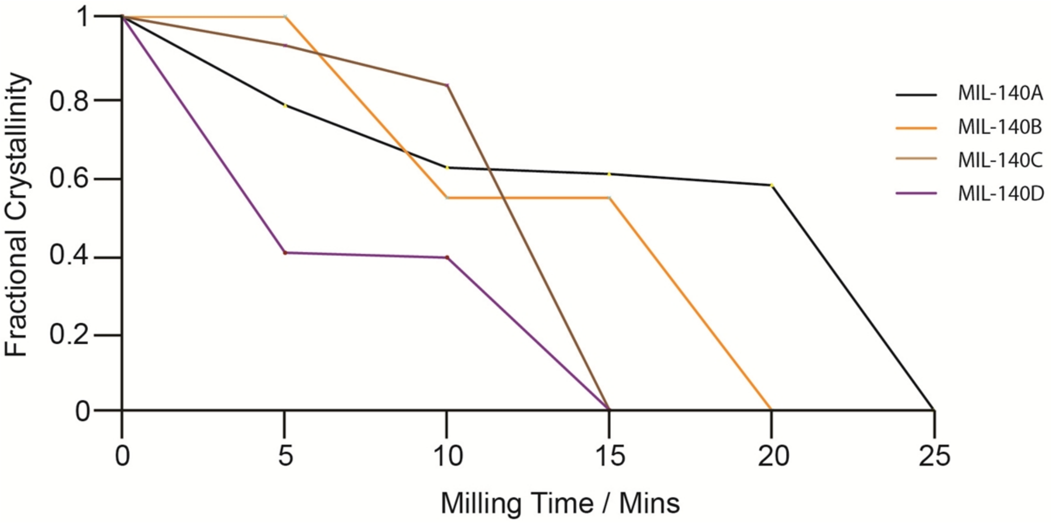

Figure S2l. Evolution of the integral breadth of the last remaining diffraction peak for MIL-140A-D.

SI-3: Scanning electron microscopy (SEM)

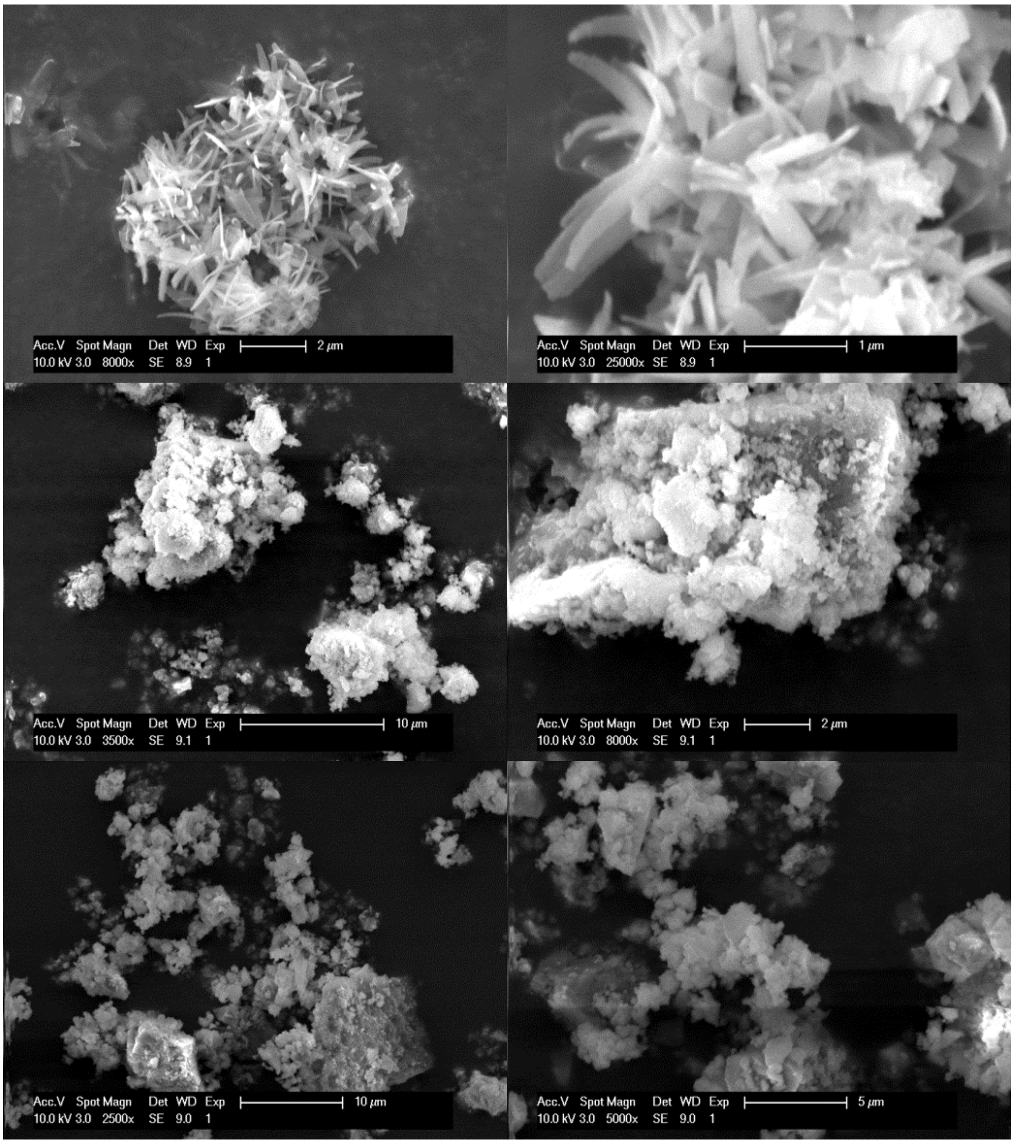

Figure S3a. SEM images of samples of MIL-140A. Top – crystalline, middle – after ten minutes of ball-milling and bottom – after 25 minutes of ball-milling.

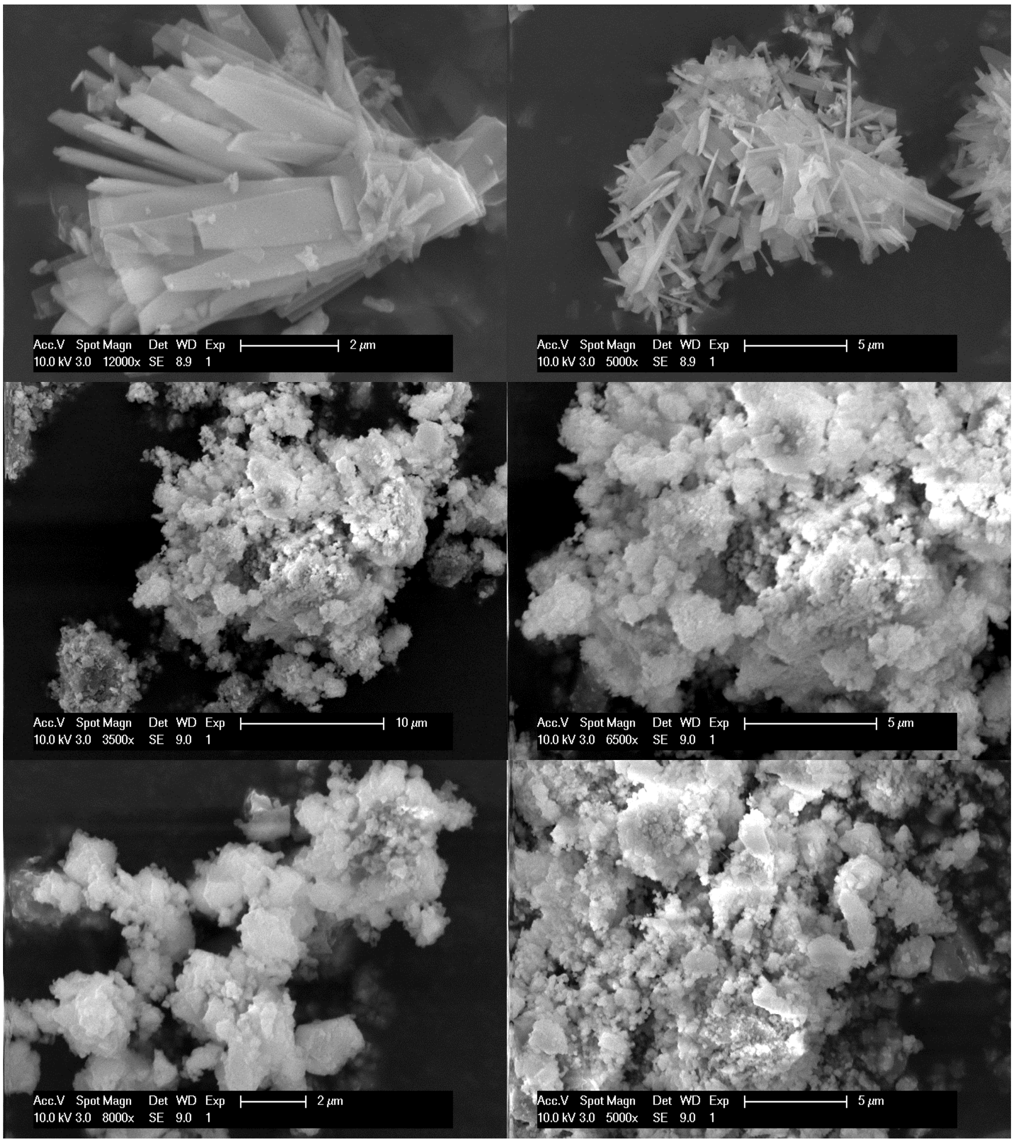

Figure S3b. SEM images of samples of MIL-140B. Top – crystalline, middle – after ten minutes of ball-milling and bottom – after 25 minutes of ball-milling.

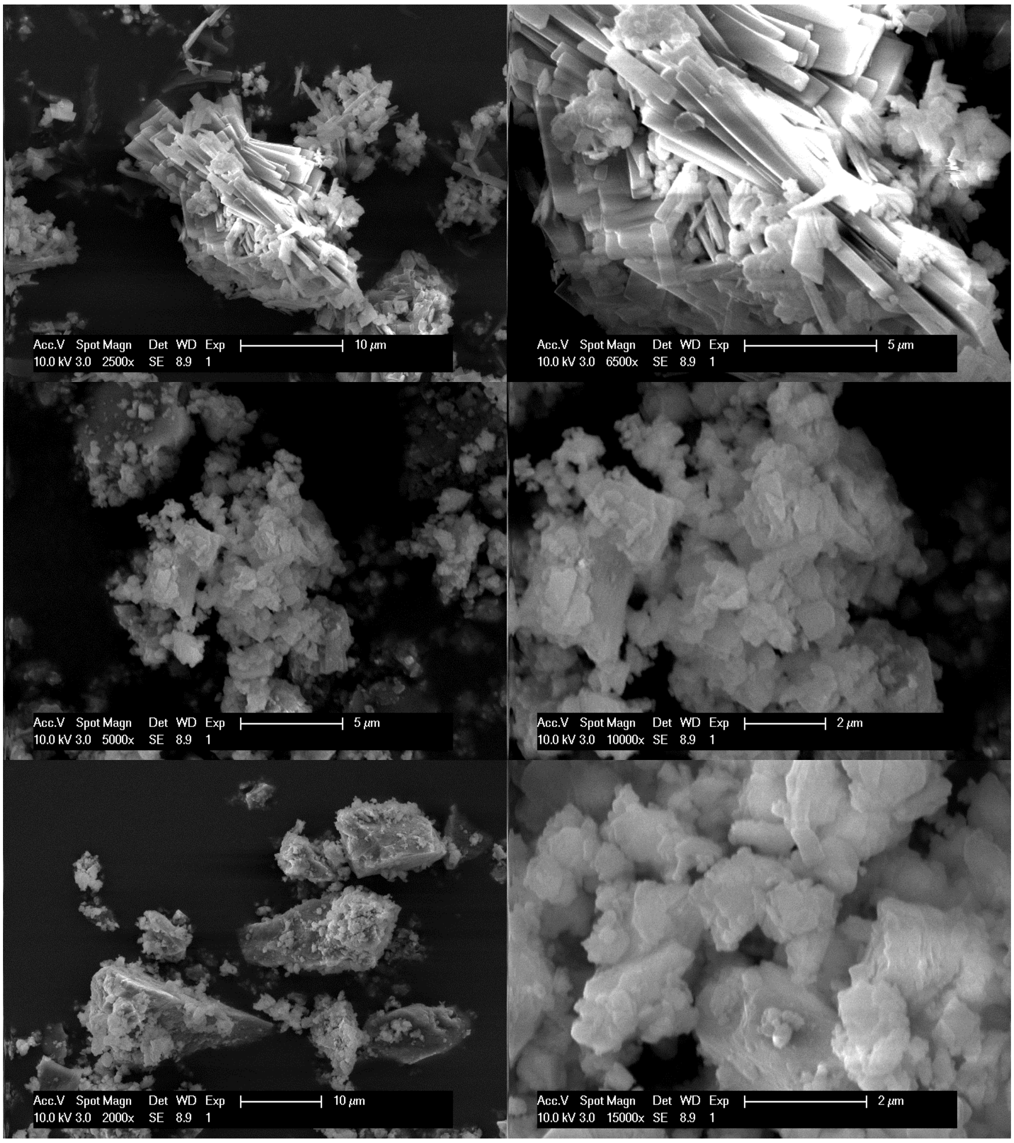

Figure S3c. SEM images of samples of MIL-140C. Top – crystalline, middle – after ten minutes of ball-milling and bottom – after 25 minutes of ball-milling.

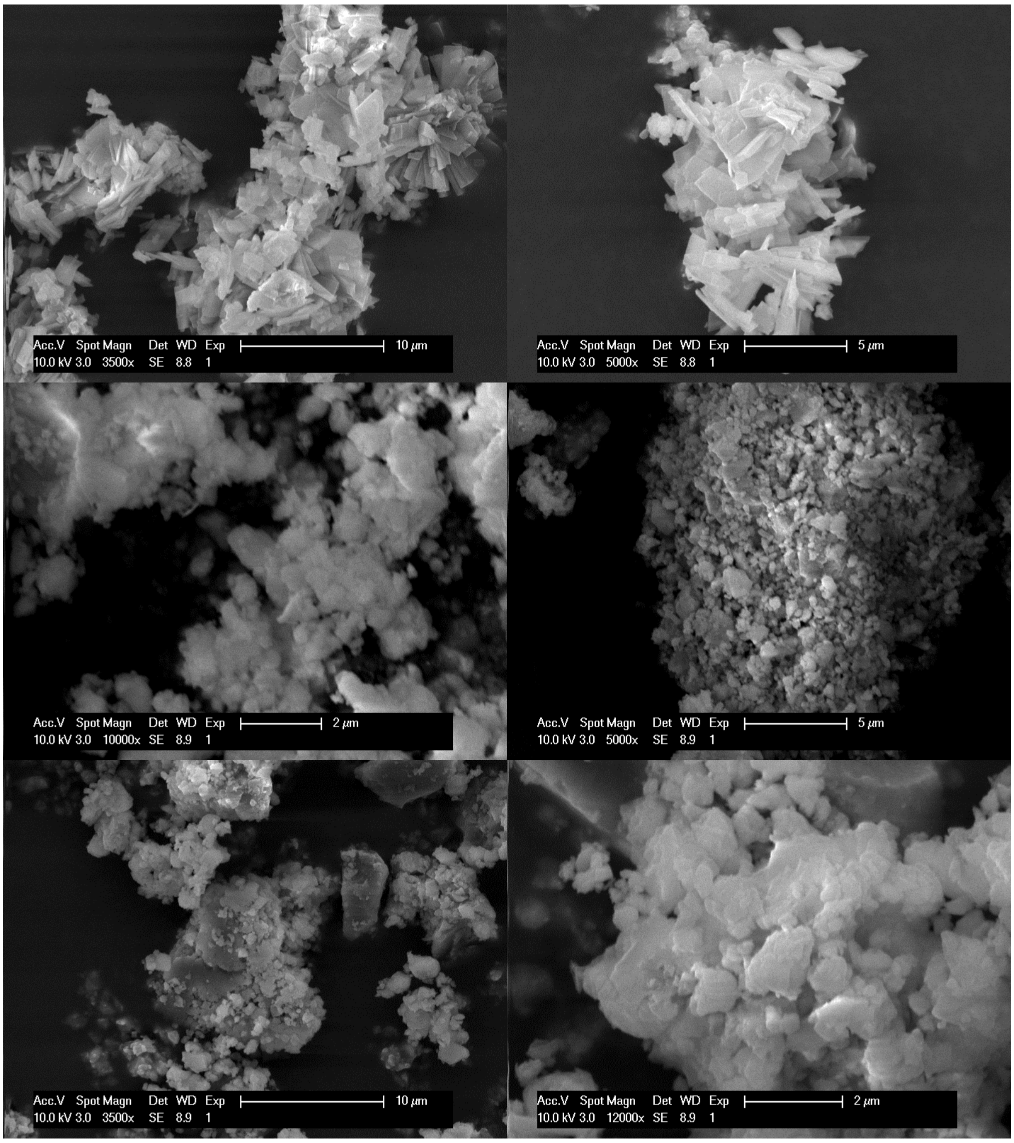

Figure S3d. SEM images of samples of MIL-140D. Top – crystalline, middle – after ten minutes of ball-milling and bottom – after 25 minutes of ball-milling.

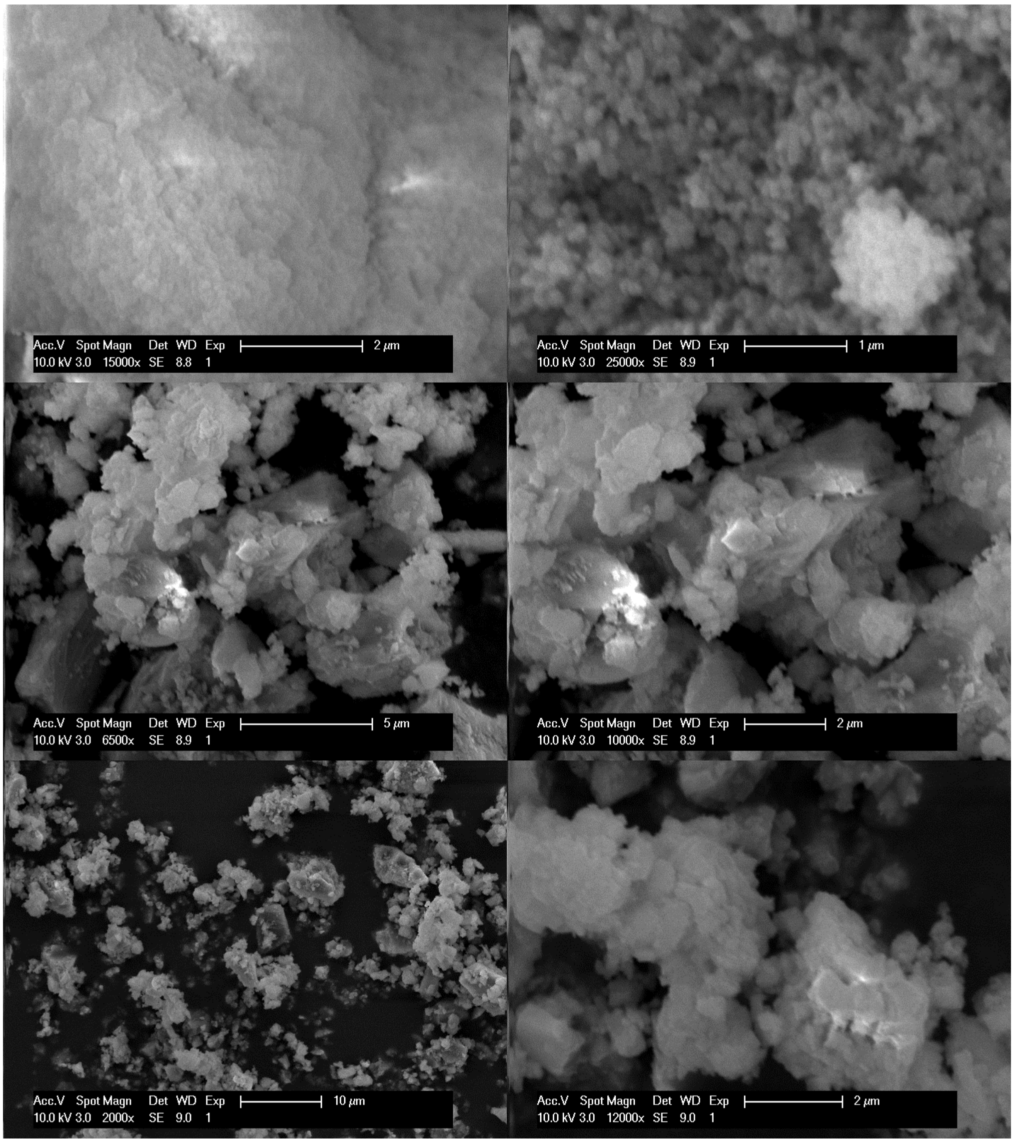

Figure S3e. SEM images of samples of UiO-66. Top – crystalline, middle – after ten minutes of ball-milling and bottom – after 25 minutes of ball-milling.

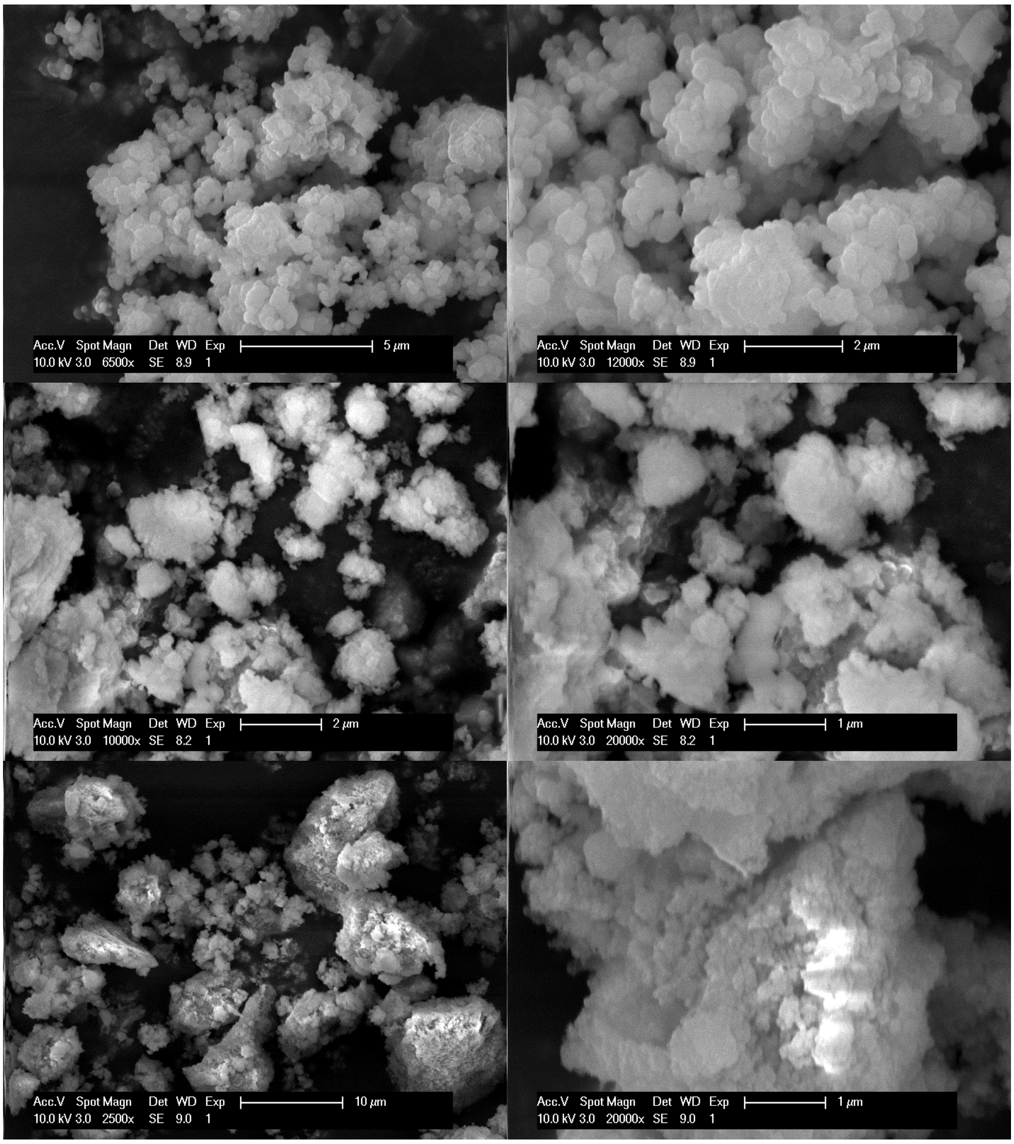

Figure S3f. SEM images of samples of UiO-66m TFA. Top – crystalline, middle – after ten minutes of ball-milling and bottom – after 25 minutes of ball-milling.

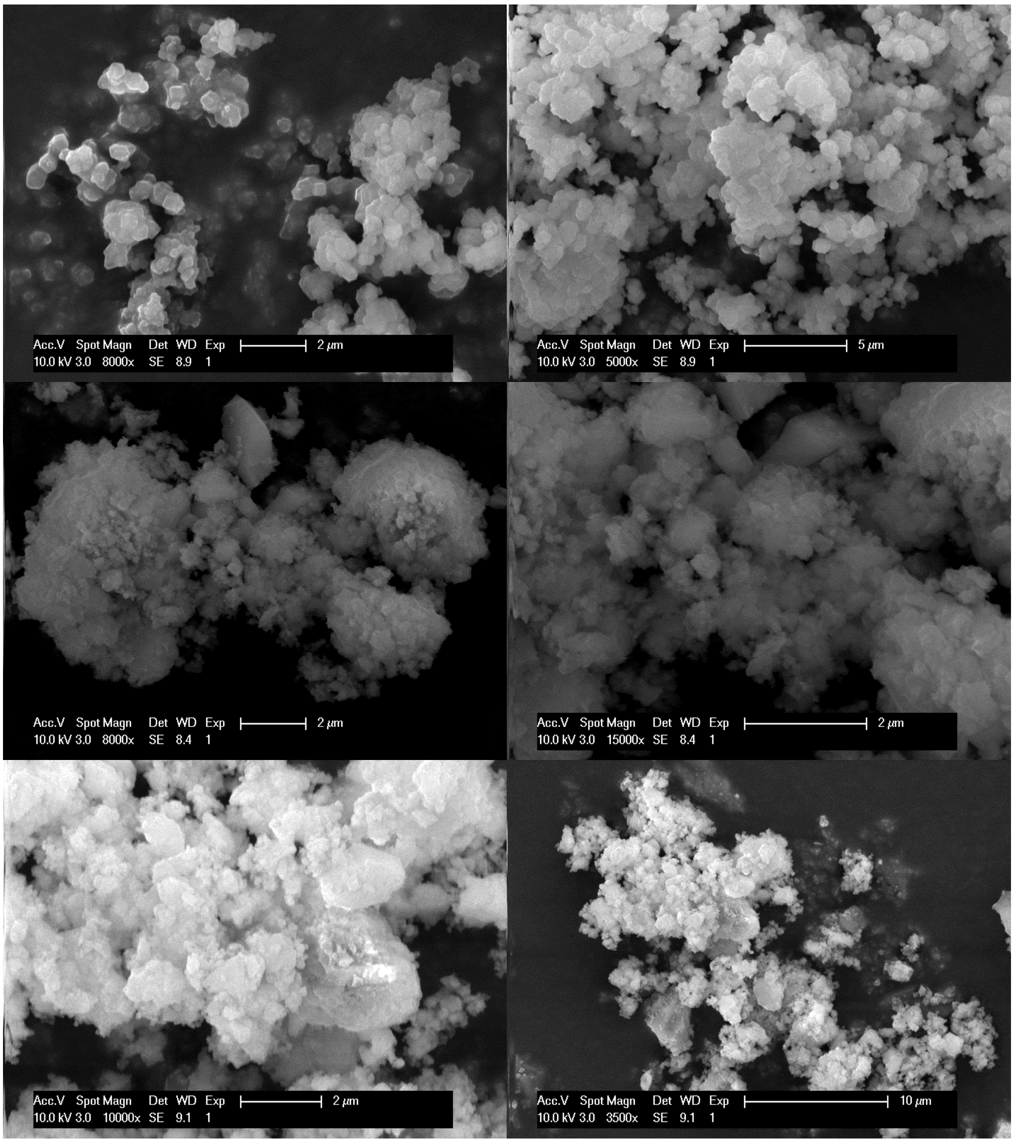

Figure S3g. SEM images of samples of ZIF-8. Top – crystalline, middle – after ten minutes of ball-milling and bottom – after 25 minutes of ball-milling.

SI-4: Modulator removal from UiO-66m TFA

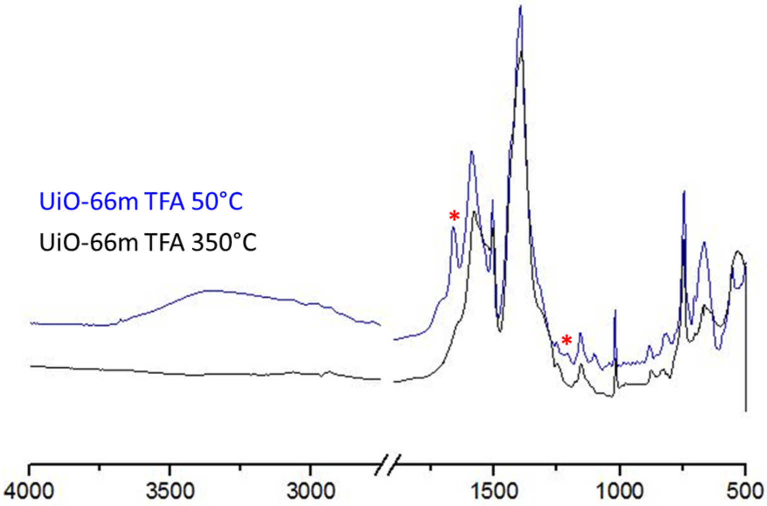

Figure S4a. Normalized FTIR spectra of UiO-66m TFA at 50°C (blue) and UiO-66m TFA at 350°C (black). The stars indicate typical vibrational signals for trifluoroacetate.

By treating UiO-66m TFA for several hours at 350°C, TFA is removed from the cluster. The material is designated as UiO-66mh, and was as well subjected to the milling treatment. The infrared spectra indicate the removal of TFA for the most characteristic peaks after a thermal treatment at 350°C as indicated by the red stars.

SI-5: N_2 physisorption and pore size distribution analysis

It is important to note that the pore-size distributions were calculated with the Tarazona NLDFT model using a regularization factor 0.00100. This model is not specific for MOF structures, however the qualitative analysis of the PSD’s is correct.

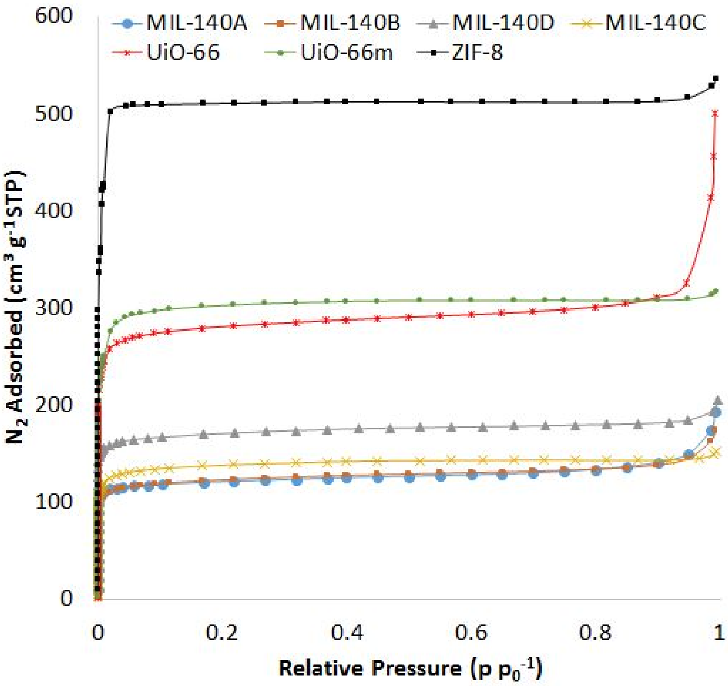

Figure S5a. N_2 physisorption isotherms for the crystalline MIL-140(A-D), UiO-66, UiO-66m TFA and ZIF-8.

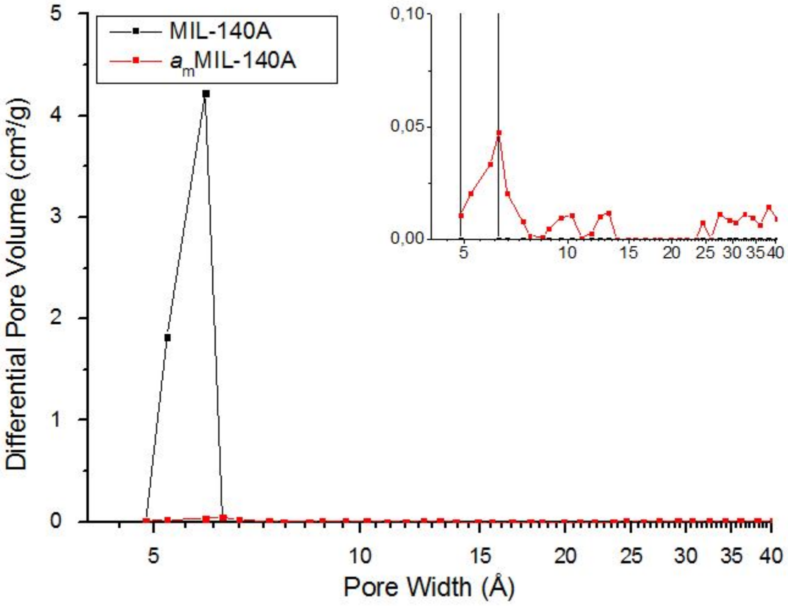

Figure S5b. Pore size distributional analysis for crystalline (black) and amorphized (red) MIL-140A.

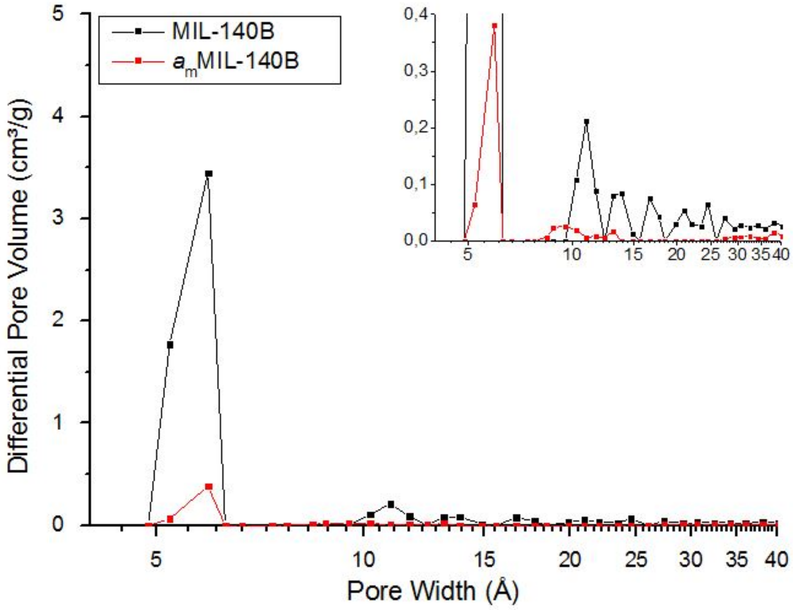

Figure S5c. Pore size distributional analysis for crystalline (black) and amorphized (red) MIL-140B.

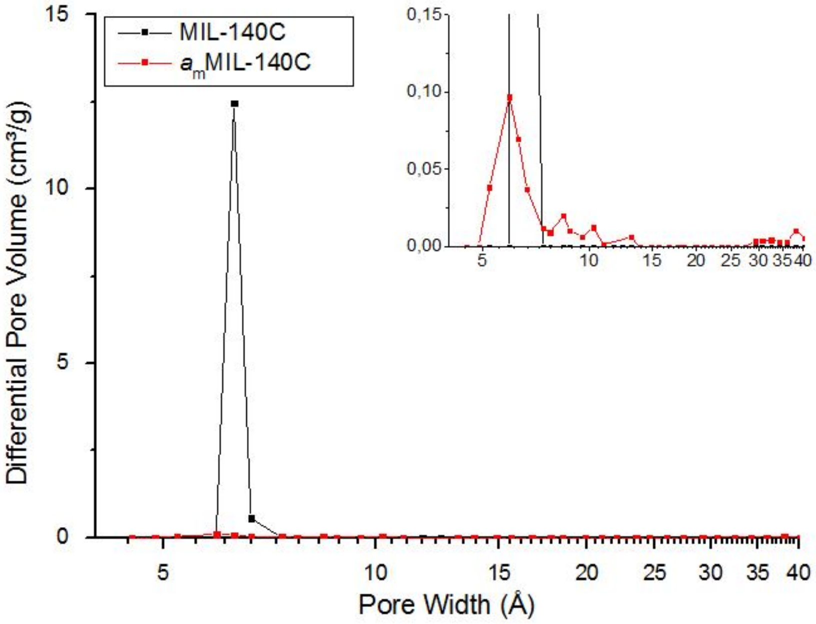

Figure S5d. Pore size distributional analysis for crystalline (black) and amorphized (red) MIL-140C.

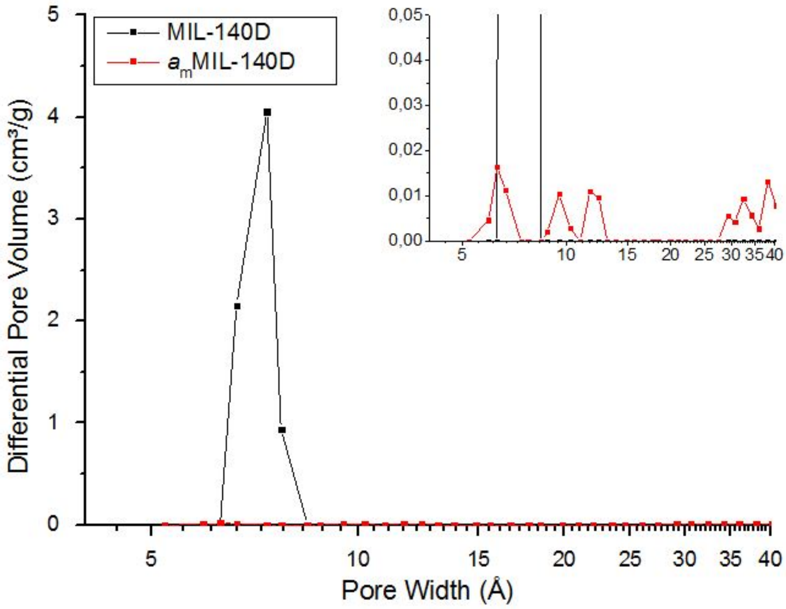

Figure S5e. Pore size distributional analysis for crystalline (black) and amorphized (red) MIL-140D.

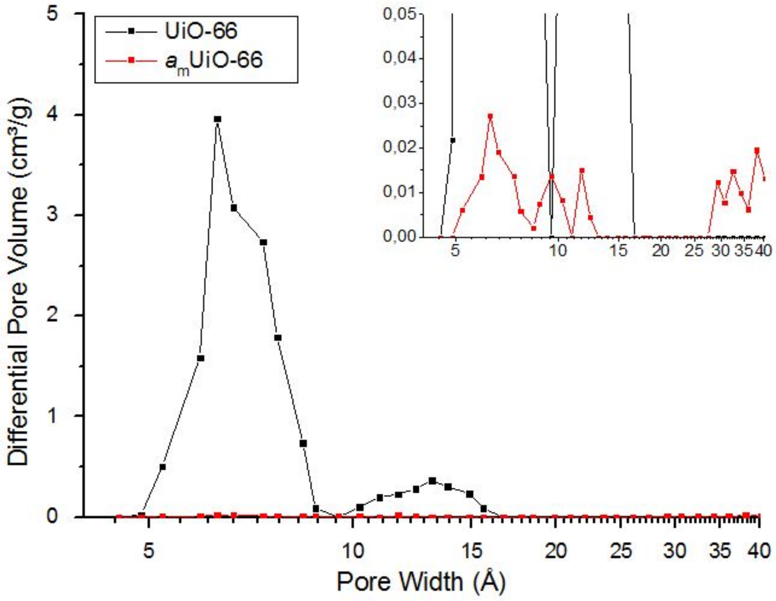

Figure S5f. Pore size distributional analysis for crystalline (black) and amorphized (red) UiO-66.

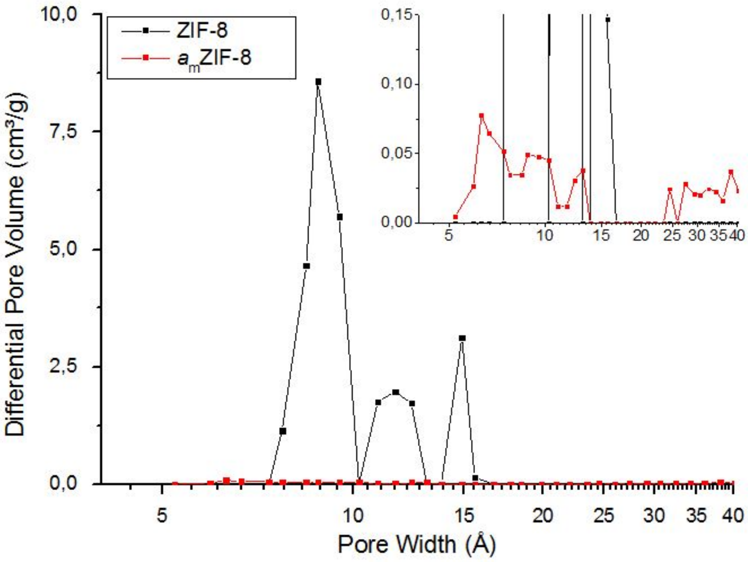

Figure S5g. Pore size distributional analysis for crystalline (black) and amorphized (red) ZIF-8.

SI-6: Thermogravimetric Analysis

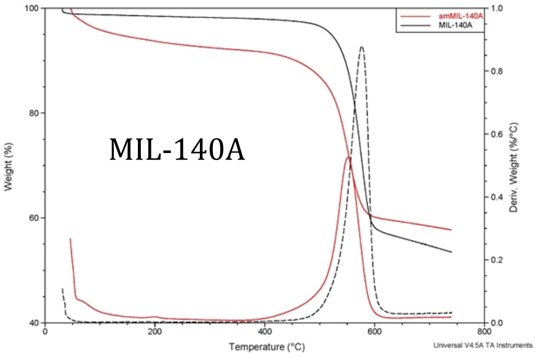

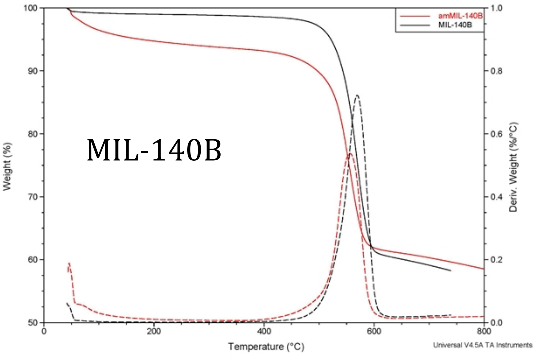

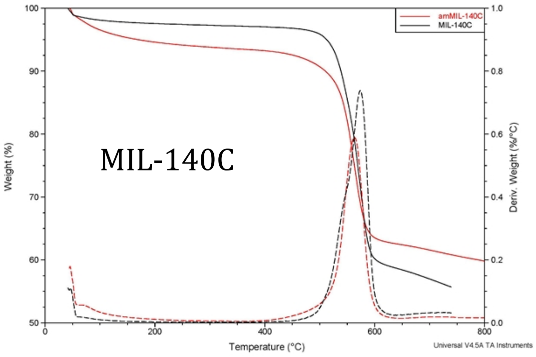

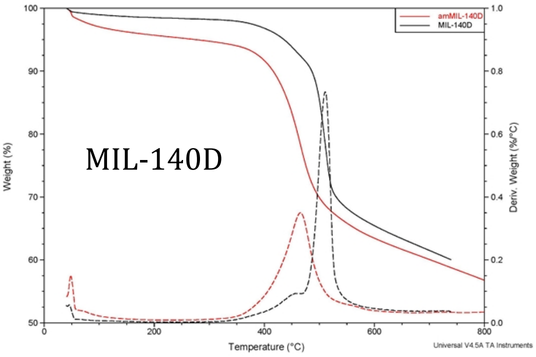

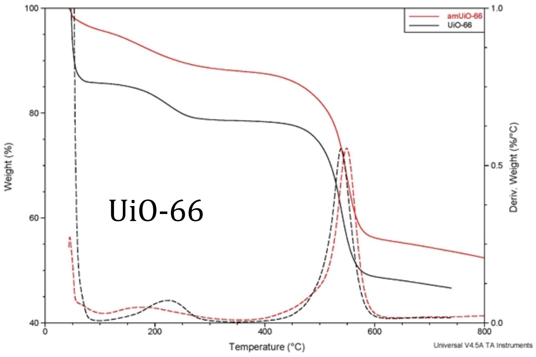

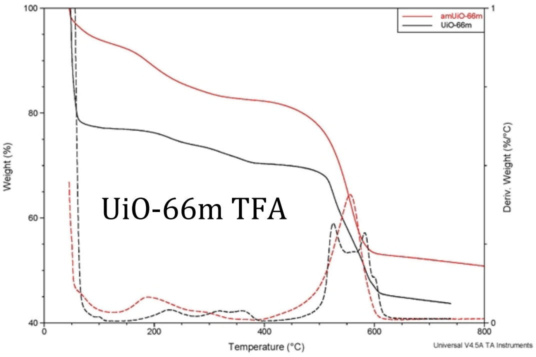

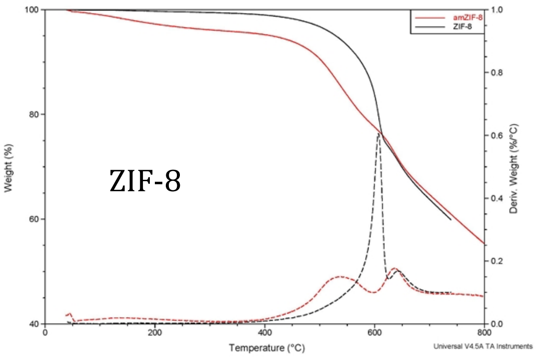

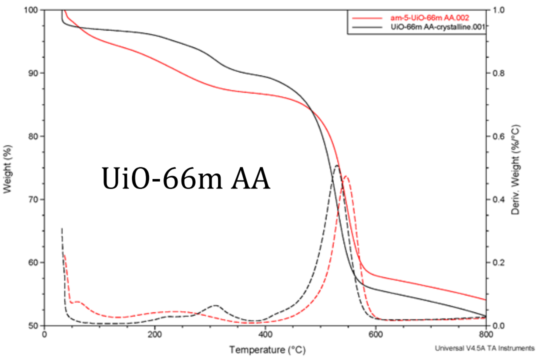

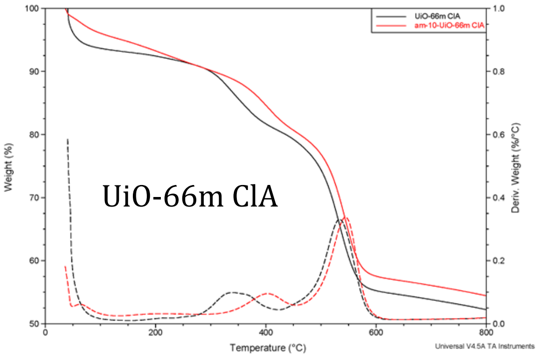

Figure S6a. Thermogravimetic TGA) traces under N_2 atmosphere (solid lines) and derivative TGA curves (dashed lines) of crystalline (black) and amorphous (red) samples of the zirconium containing frameworks studied, along with ZIF-8.

SI-7: IR spectroscopy

All samples were outgassed at 50°C under vacuum unless otherwise indicated. The absorbance is normalised for all spectra. Slight variance from the results in Figure 5 arises from slightly different outgassing procedures.

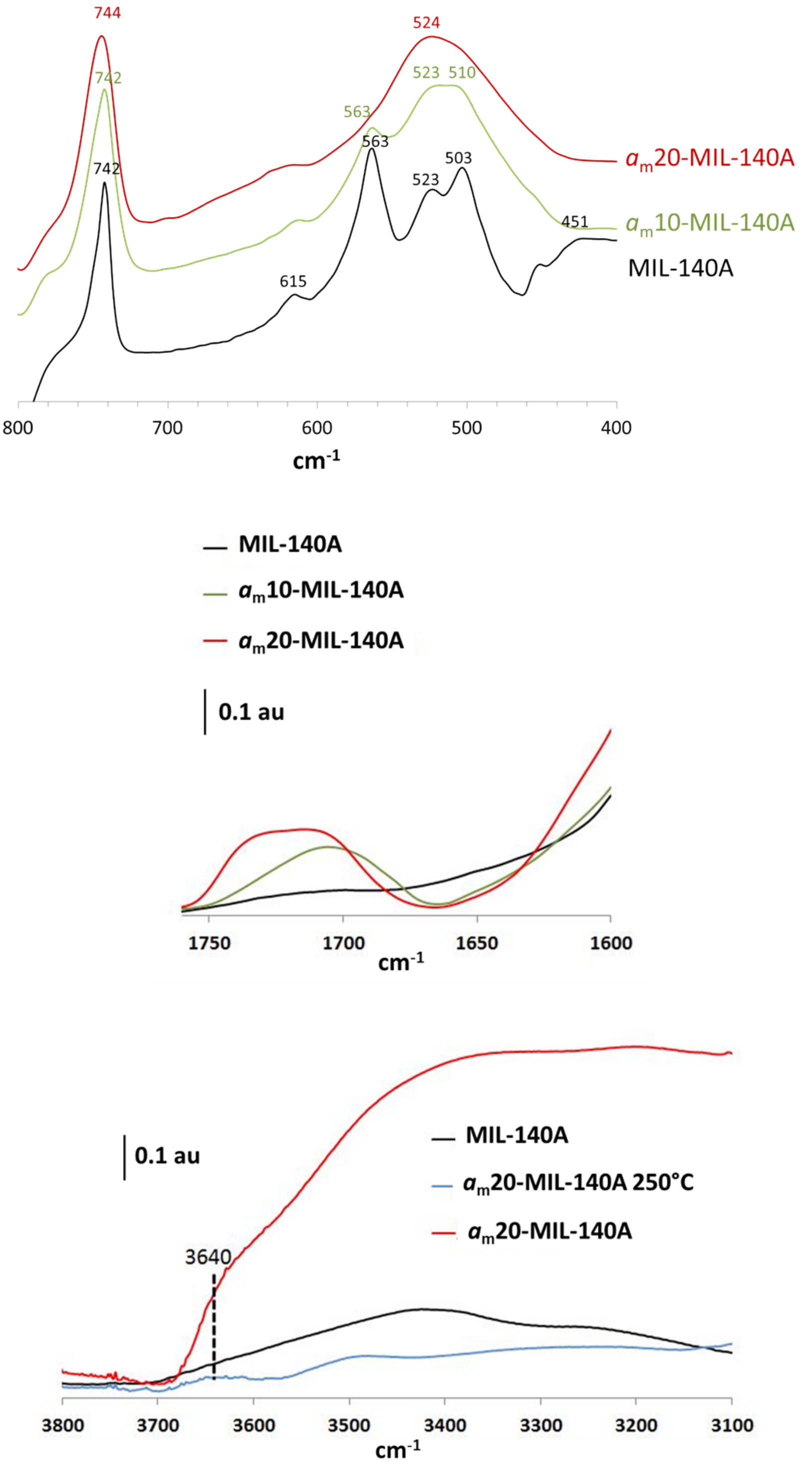

Figure S7a. Infra-red spectroscopy spectra for MIL-140A and the amorphized framework for the regions (top) 400-800 cm^{-1}, (middle) 1600-1800 cm^{-1} and (bottom) 3100-3800 cm^{-1}.

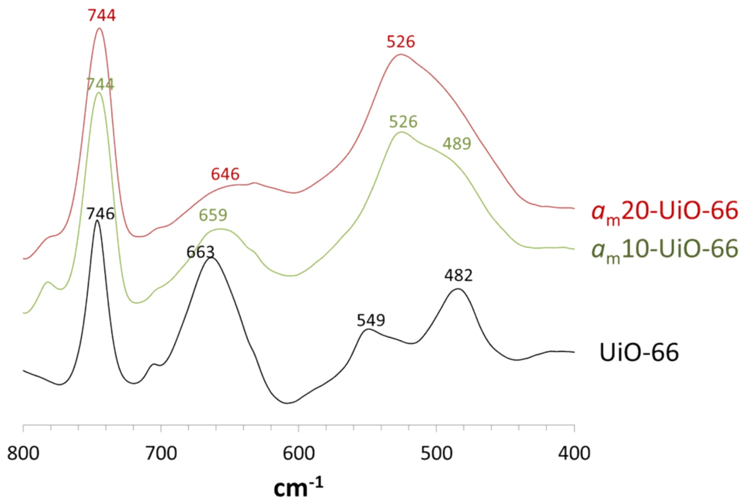
744
526
744
526
489
646
659
746
663
482
549
a_m20-UiO-66
a_m10-UiO-66
UiO-66
800
700
600
500
400
cm^{-1}

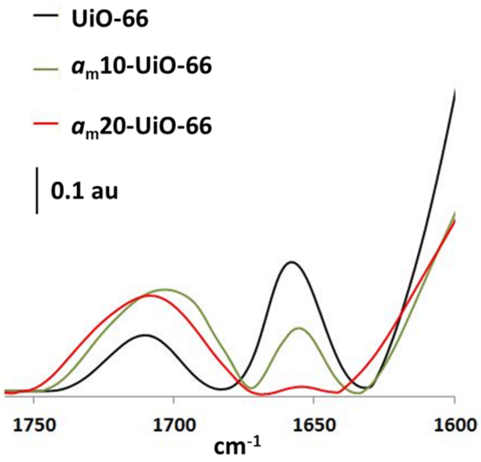
UiO-66
a_m10-UiO-66
a_m20-UiO-66
0.1 au
1750
1700
1650
1600
cm^{-1}

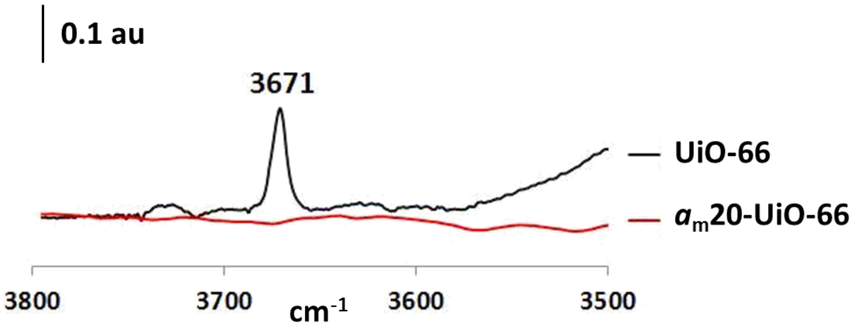
0.1 au
3671
UiO-66
a_m20-UiO-66
3800
3700
cm^{-1}
3600
3500

Figure S7b. Infra-red spectroscopy spectra for UiO-66 and the amorphized framework for the regions (top) 400-800 cm^{-1}, (middle) 1600-1800 cm^{-1} and (bottom) 3100-3800 cm^{-1}.

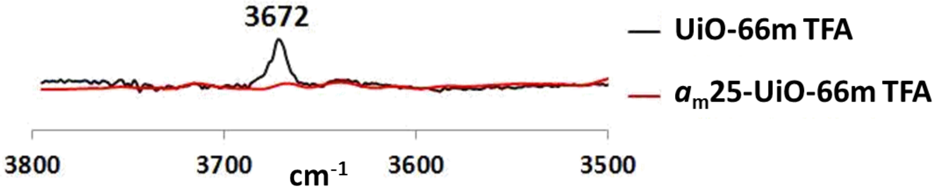

Figure S7c. Infra-red spectroscopy spectra for UiO-66m TFA and the framework after 25 minutes of ball-milling for the regions (top) 400-800 cm^{-1}, (middle) 1600-1800 cm^{-1} and (bottom) 3100-3800 cm^{-1}.

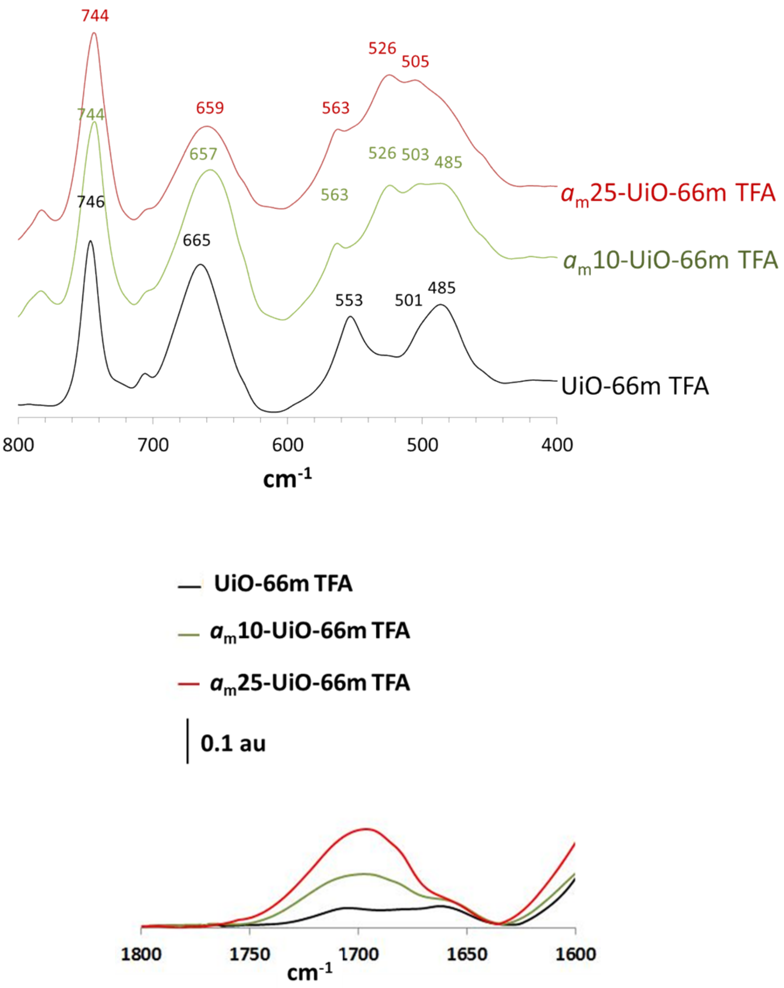
744
526
505
659
563
744
657
526 503
485
746
563
665
553
501
485
a_m25-UiO-66m TFA
a_m10-UiO-66m TFA
UiO-66m TFA
800
700
600
500
400
cm^{-1}
UiO-66m TFA
a_m10-UiO-66m TFA
a_m25-UiO-66m TFA
0.1 au
1800
1750
1700
1650
1600
cm^{-1}